Marine Geology, 64 (1985) 91—111
Elsevier Science Publishers B.V., Amsterdam — Printed in The Netherlands

THEORETICAL AND OBSERVATIONAL ESTIMATES OF NEARSHORE BEDLOAD TRANSPORT RATES

M.R. GOUD and D.G. AUBREY
Woods Hole Oceanographic Institution, Woods Hole, MA 02543 (U.S.A.)

(Received January 4, 1984; revised and accepted June 11, 1984)

ABSTRACT

Goud, M.R. and Aubrey, D.G., 1985. Theoretical and observational estimates of nearshore bedload transport rates. Mar. Geol., 64: 91—111.

Sediment transport rates in a shallow (<3 m) nearshore region are estimated using theoretical models and using bedform migration rates measured from vertical aerial photographs covering a 10-yr interval. Aerial photographs of the study area in Nantucket Sound, Massachusetts, showed low-amplitude (tens of centimeters), long wave- and crest-length (tens to hundreds of meters), shore-normal sand waves in distinct geometrical patterns. The waves migrated an average of 10—20 m yr^{-1} over a 10-yr period; the migration distances and bedform dimensions were used to calculate an average volume transport rate for the area. This rate was compared to bedload transport rates calculated using a Meyer-Peter and Müller model and a Bagnold model; field observations of steady currents and directional waves provided data for the calculations. Theoretical rates based solely on asymmetrical tidal currents are as much as an order of magnitude smaller than the observed rates, but inclusion of storm wave effects in the theoretical predictions brings them into better agreement with observations. This suggests that even in tidally dominated, protected regions with low background wave energy, infrequent storm wave events significantly modify sand transport rates and patterns.

INTRODUCTION

Studying the transport of sediment in the nearshore and shelf environment raises problems of both theoretical and practical interest. In practice, problems of contaminant dispersal, coastal erosion and seafloor stability require an understanding of sediment transport processes and this need has generally been met through empirical studies. Theoretical advances in the study of interactions between a movable bed and a fluid flow, however, have provided new and effective tools for modeling sediment transport processes in natural environments (e.g., Smith, 1977; Grant and Madsen, 1979). Aspects of these theoretical approaches can be combined with field observations and empirical transport formulas to improve the understanding of sediment transport processes in the natural environment.

Direct measurement of marine sediment transport is difficult and investigators have used a variety of techniques: dyed sand (e.g., Komar and Inman, 1970), radioactive tracers (e.g., Heathershaw, 1981) and bedform migration,

0025-3227/85/$03.30

monitored with bathymetric profiles (Aubrey, 1979) or stake fields (e.g., Salsman et al., 1966). The difficulty of monitoring the small changes in these transport indicators limits these studies to short time durations and small areal extent. Transport rates evaluated in these types of studies are time-averaged measures of the response of the bed to the flow and can be generalized only in so far as the flow conditions during the period of study can be assumed to be typical of a longer time duration and a larger area.

Transport estimates can also be made with a more dynamically oriented approach: measure the physical forcing mechanisms (i.e., waves and currents) in the marine environment, employ fluid dynamical theory to convert these records into bottom shear stress estimates and use empirical models to calculate sediment transport rates. This method overcomes some of the problems of direct measurement, since the estimates are derived from the area's flow field and seafloor configuration. The flow field can be easily measured over relatively long periods (months or years) or extrapolated from long-term weather records; the seafloor configuration can be characterized using samples, bathymetric profiles, photographs or direct observations. However, uncertainties in calculating boundary shear stress based on point velocity measurements in the water column and lack of field corroboration for flume-derived sediment transport formulas make this approach unreliable in practice, even in steady-flow environments where the bed configuration is constant. Introduction of surface gravity waves and a movable bed makes sediment transport calculations even more suspect. The empirical transport formulas themselves were derived from steady-flow flume experiments and have undergone only limited testing in the field.

The uncertainties in the calculations are obvious when the method is applied. Gadd et al. (1978) compared three bedload transport formulas (disregarding suspended load) in a tidally dominated region and found an order of magnitude difference in the predicted transport rates. Heathershaw (1981) compared predicted transport with sand movement measured using radioactive tracers; the predicted direction of transport coincided with the observed, but with a large variation between estimates of transport rates. The variations between the theoretical estimates in these results emphasize the necessity for field experiments to constrain the theoretical approach.

This study compares sediment transport predictions based on current-meter records and bedload formulas with transport calculated from sand-wave migration distances. Use of aerial photographs to measure sand-wave movement makes possible an unusually long time scale since photographic coverage spanned ten years. High-frequency surface gravity waves are shown to be important for sediment transport, even in a shallow, tidally dominated nearshore region.

STUDY AREA

Sediment transport was examined on a shallow platform (<3 m in depth) extending one kilometer offshore from Popponesset Beach on Cape Cod, Mass. (Fig.1). The platform is located in Nantucket Sound between Cape Cod and nearby islands. The bathymetry of the Sound is a complex configuration of shoals and channels, which complicates tidal flow patterns and, with the sheltering effect of the islands, protects the study area from open ocean swell.

The area of interest, referred to here as Popponesset Platform, is wedge-shaped, extending for 5 km along the shoreline from Succonesset Point northeast to Meadow Point (Fig.1). Its seaward limit is defined by a steep slope towards a channel which reaches depths of 11 m. The channel is less than 3 km wide, shoaling rapidly to a linear ridge (Succonnesset Shoal). A set of nearly shore-normal sand waves, easily distinguished on aerial photographs (Fig.2), cover the platform. Wavelengths and crestlengths are on the order of tens to hundreds of meters, and soundings showed the waves range from 30 to 60 cm in height, with gently sloping, near-flat stoss slopes and relatively steep lee slopes (Fig.3).

Photographs taken in successive years clearly show the sand waves migrating slowly toward the southwest (Fig.4); the pattern of southwest migration is also evident over time periods up to three decades (Fig.5). Tidal flows on the platform generally parallel the shoreline and non-storm wave energy is insignificant. Because of this, little on-offshore sediment exchange takes place.

METHODS

A detailed net of sounding lines was run to determine the general bathymetry of the region (Fig.6) and the dimensions of the sand waves. Bathymetry was acquired using a 200 kHz Raytheon DE719C precision echo sounder, corrected for tides as measured at the time of the surveys. Navigation was performed with a Del Norte Trisponder microwave navigation system with three shore-based transponders providing ranges to the vessel. Precision is within 5 m (root-mean-square error).

Distances of migration of the sand waves, measured from high precision, map quality vertical aerial photographs, average 10—20 m yr^{-1} over the period 1971—1981. Series of photographs at a scale of 1:18,000 were taken on four separate dates between August 1981 and October 1982 as a part of this study. Migration distances from 0 to 30 m are visible over that year (Fig.4). A set of photos taken in 1971, archived at the U.S. Department of Agriculture, provided data for longer term migration rate measurements (Fig.5). Forty-three sets of aerial photos have been taken of this area between 1938 and the present (Aubrey and Gaines, 1982) and platform sand wave patterns are visible on most of them. However, variable migration rates, differences in photo scales and poor photo quality before 1970 make

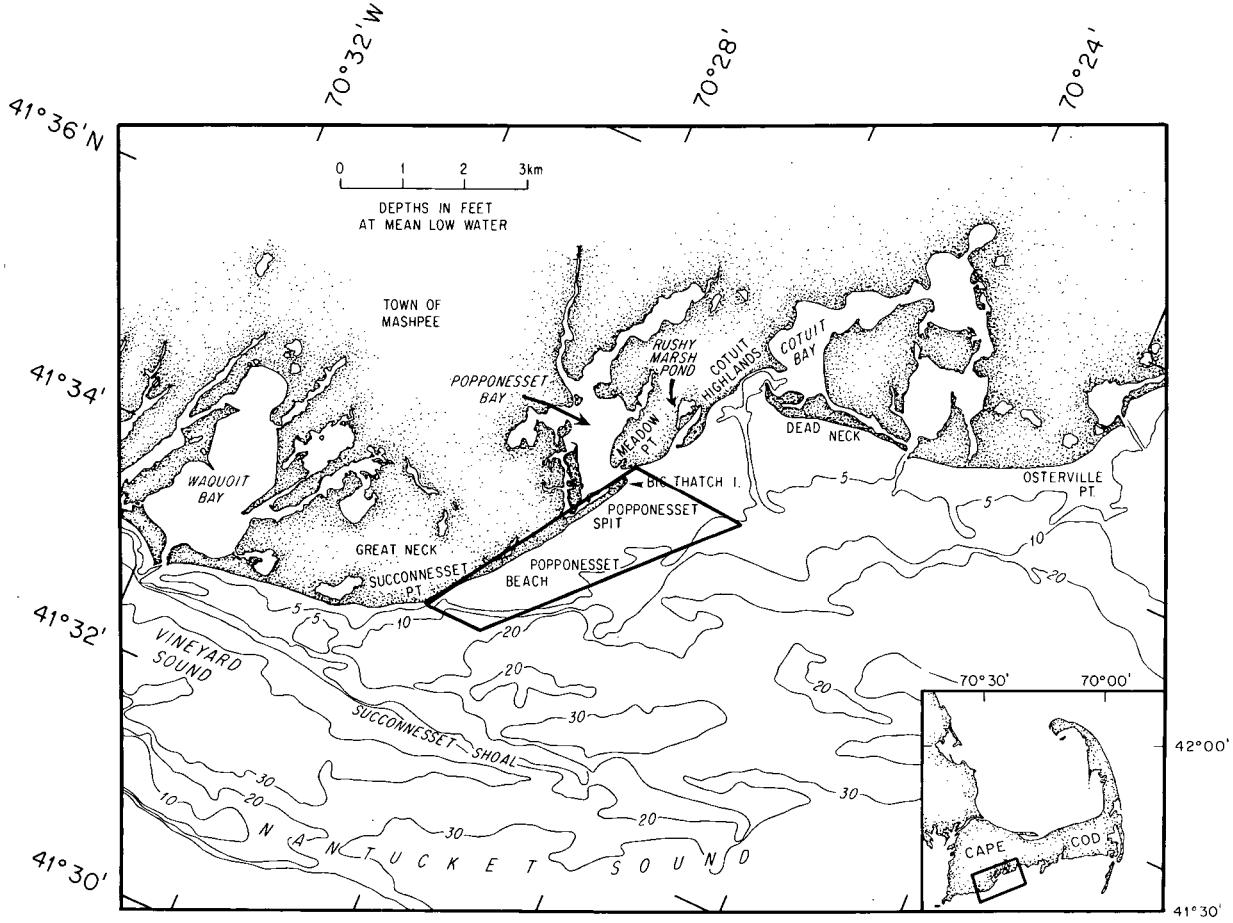

Fig.1. The Popponesset barrier beach setting, Cape Cod, Mass. Popponesset Platform is enclosed in box.

Fig.2. Aerial photograph of study area, showing sand waves on Popponesset Platform. Photo taken 19 August 1981.

correlation of individual sand waves impossible beyond the ten-year interval 1971—1981, limiting the study to that period.

Grain-size characteristics used in the sediment transport formulas are determined from 27 surface sediment samples from the platform (Fig.7). Samples were collected using a hand-operated grab sampler and analyzed for grain-size distribution using an electronic settling tube (Schlee, 1966). All samples were fine-to-coarse, abiotic sand with negligible silt- or clay-sized

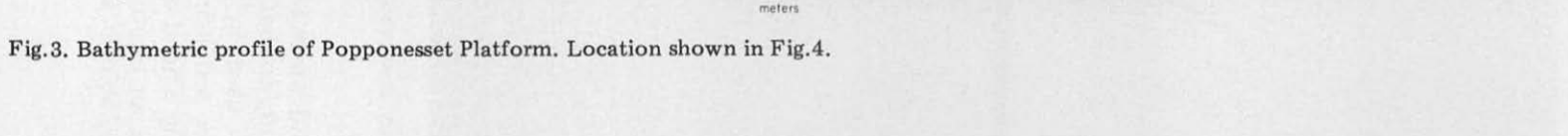

Fig. 3. Bathymetric profile of Popponesset Platform. Location shown in Fig. 4.

Fig.4. Sand-wave migration patterns on Popponesset Platform for the period 1981—1982. Location of profile in Fig.3 is shown.

components and little or no gravel. Median grain sizes (Fig.7), calculated using graphic moments techniques (Inman, 1952), ranged from 26 to 67 μm. Eigenfunction analysis of the grain-size classes of all 27 samples gave a mean grain size for the platform of 35 μm, and this value was used in transport calculations (for details of the eigenfunction analysis, see Aubrey and Goud, 1983). The low volume of silt and clay and lack of biological activity allowed an assumption of cohesionless transport. Sediment grain density is assumed to be 2.65 g cm^{-3}.

Two current meter deployments were made in the study area during the fall of 1982. A Neil Brown two-axis acoustic current meter, sampling at a 10-s interval, was located on the platform from 22 October through 9 November (Fig.7). Water depth was approximately 2.5 m with the sensor 1.5 m above the bottom. The second set of current measurements was part of a wave gage deployment in 6.5 m of water in the channel (Fig.7) from 2 November through 30 November, 1982. The instrument was a Sea Data 635-12 wave gage, which consists of a two-axis electromagnetic current sensor located 1.98 m above the bottom and a precise quartz oscillator

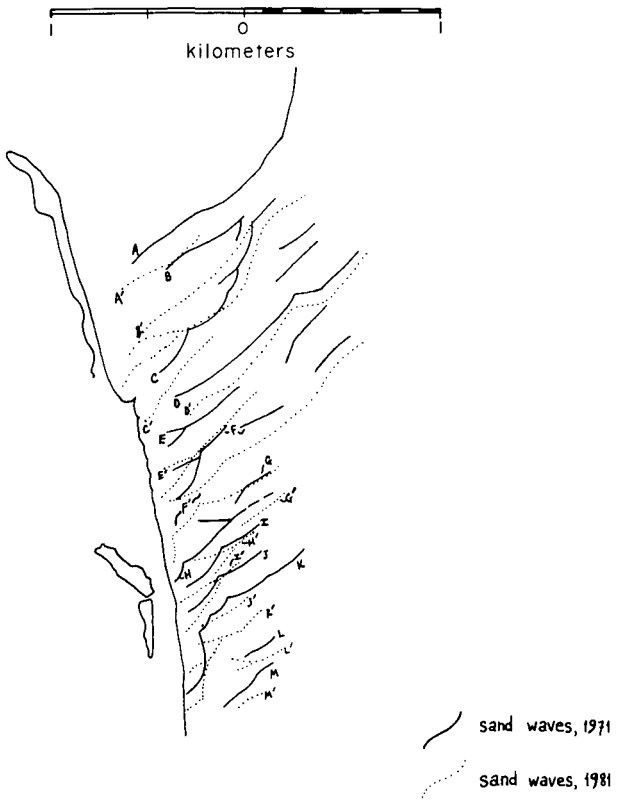

Fig.5. Sand-wave migration patterns on Popponesset Platform for the period 1971—1981.

pressure sensor, internally recording. The instrument sampled flows continually at 30-min intervals, with burst sampling every four hours at a 1-s rate for 2064 s.

Both records showed a strongly rectilinear, semi-diurnal tidal flow parallel to the coast. Channel flow direction was 45° TN (clockwise from true north) on flood tide and 225°TN on ebb. A rotary component spectral analysis (Gonella, 1972) of the platform tidal data gave an ellipse orientation of 217° TN for all tidal components and practically no shore-normal flow. Flows in the channel were generally faster than on the platform: there the root-mean-square amplitude of the tidal flows was approximately 41 cm s^{-1}. On the platform the rms amplitude was 34 cm s^{-1} and flow velocities reached 40 cm s^{-1} less than 2% of the time (Fig.8). Net tidal asymmetries to the southwest were observed in both records; asymmetries in speed and duration of the flows are responsible for net sediment transport.

Wave energy was low during the month of deployment, with an average sea surface variance $\langle \eta^2 \rangle$ of only 61 cm^2, calculated from measurements of the free surface from mean sea level (η) due to surface gravity waves. Variance is related to the total wave energy per unit area (E) by the equation:

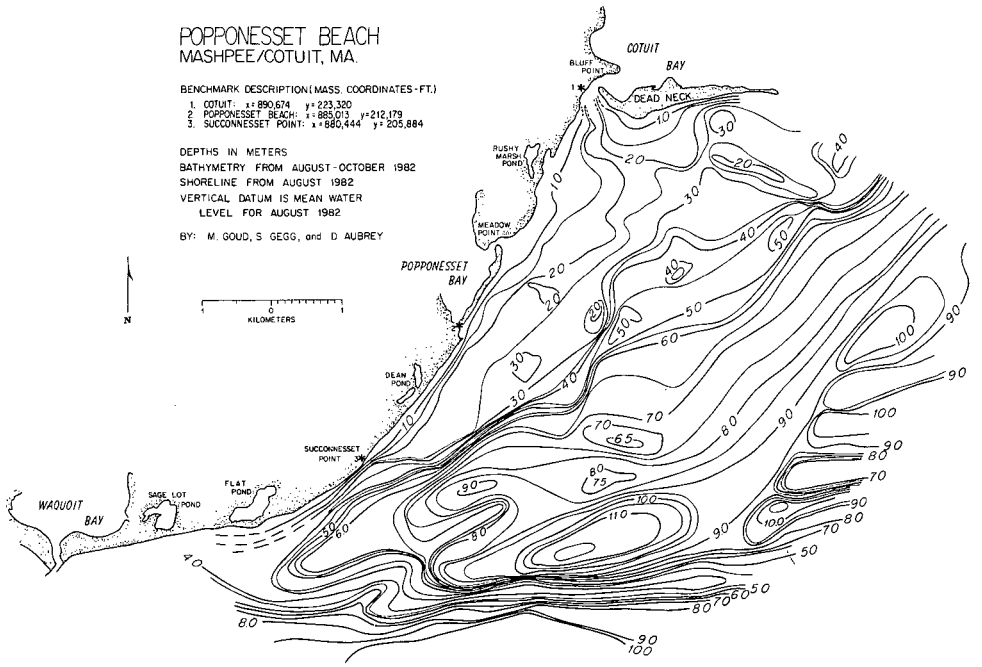

Fig. 6. Detailed bathymetric map of the Popponesset Beach region.

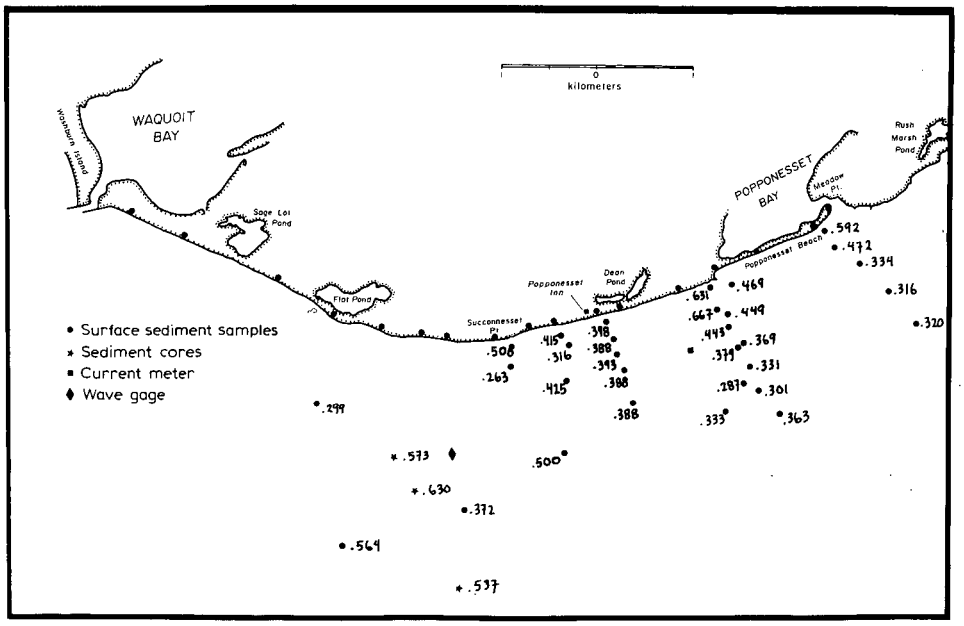

Fig. 7. Locations and median grain size of surface sediment samples and locations of instruments deployed (grain size in mm).

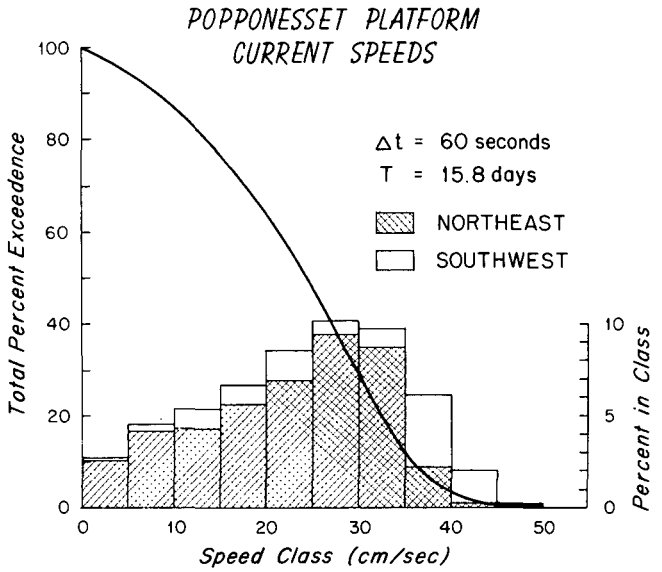

Fig.8. Histogram of tidal currents during current meter deployment on Popponesset Platform. Percent in speed class in a particular direction is indicated by upper limit of appropriate pattern. T = record length; Δt = period over which 10-s samples were averaged.

$$E = \rho g \langle \eta^2 \rangle$$

where ρ is the density of water and g is gravitational acceleration. Another representation of wave energy, significant wave height ($H_{1/3}$), is the mean height of the highest one third of the waves and is close to the wave height one would estimate visually. It is approximated as:

$$H_{1/3} = 4\sqrt{\langle \eta^2 \rangle}$$

For the period of the study, mean significant wave height was only 24 cm and the mean peak period was between three and four seconds. Waves in this range will have a non-linear reaction with the tidal current to enhance boundary shear stress (Grant and Madsen, 1979) and thus increase sediment transport. These small waves, however, add only minimally to the total bottom stress: the enhanced shear velocity (u_*) is at most 15% greater than that calculated from the current alone. This falls within the range of uncertainty due to other factors (e.g., boundary roughness, skin friction/total shear-stress ratio, critical shear stress, all discussed in more detail below), so the process will be linearized to assume quasi-steady flow due to tidal currents.

Comparisons of wave and wind activity, based on hourly meteorological observations at nearby Otis Air Force Base during October and November, showed surface waves responding directly to local winds (Fig.9). Both wave energy and direction were directly correlated with winds, indicating that wave climate for this area can be estimated from local weather records,

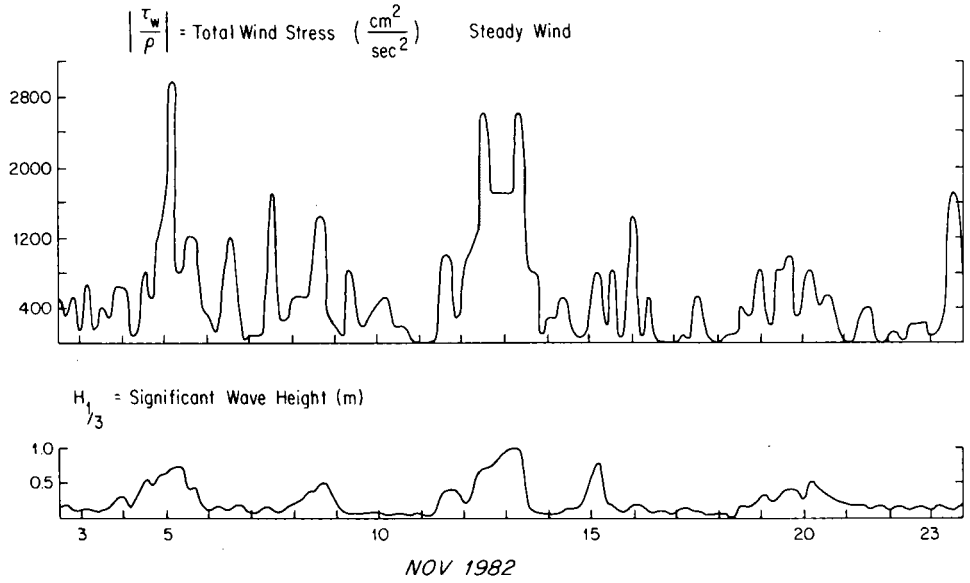

Fig. 9. Time series of significant wave height ($H_{1/3}$) and wind stress during wave gage deployment.

without consideration of open ocean swell. This observation is important for long-term estimates of sediment transport.

Maximum windspeeds during November, 1982, were about 10 m s^{-1}, generating waves with a significant height of about 1.0 m in the channel and a period of four seconds (over the fetch of Nantucket Sound). Based on shallow-water wave models, a 12.5 m s^{-1} wind would generate 1.3 m waves with a maximum period of five seconds; 1.0 m surface gravity waves would be generated on Popponesset Platform by extended periods of 7.5 m s^{-1} winds. Waves of that magnitude would affect sediment transport on the platform by greatly increasing the bottom shear stress.

RESULTS AND DISCUSSION

Volume sediment transport rates were calculated using three different methods. Net volume transport was calculated based on sand-wave migration distances; two sets of bedload transport volumes were calculated based on the platform current measurements, one using a modified Meyer-Peter and Müller (1948) equation, the other with a modified Bagnold (1963) formula. Comparison of these estimates tests the assumption that the volume of sediment transported in the sand wave can be approximated by the bedload transport estimates. This equivalence has been verified by a history of observation of bedform migration as a vehicle for bedload transport of sediment, dating from Gilbert's (1914) careful observations of sediment movement in streams and flumes. Bedforms as transport mechanisms have

been studied widely since then in both the laboratory (e.g., Simons and Richardson, 1961) and the field (e.g., McCave, 1971; Bokuniewicz et al., 1977). Since neither bedform migration nor the bedload transport equations include suspended load, both are minimum estimates of total sediment transport.

While the term *sand wave* is sometimes used to describe any periodic irregularity in a granular material from scales of centimeters to hundreds of meters (Yalin, 1972), its use here is limited to large scale bedforms which do not respond to short-period (i.e., tidal cycle) variations in the sediment flux. Smaller scale (cm) bedforms which form in response to flows only slightly greater than threshold for sediment motion will be referred to as *ripples*; they are superimposed on the large sand waves and are assumed to cover the platform. This usage is consistent with the literature for environments comparable to Popponesset Platform.

SAND-WAVE VOLUME TRANSPORT

Calculation of long-term sediment transport rates based on migration of the Popponesset sand waves required an estimate of the volume of sand within a wave. The sand-wave volume was modeled two ways. A minimum volume was calculated using the assumption that the sand movement is concentrated in the immediate vicinity of the wave crest, forming in cross section an isolated, asymmetric triangle which migrates across the flat platform (analogous in appearance to a solitary wave). A reference sand-wave volume $V_{0(\min)}$ (= volume per meter of crest length per wave length) was calculated, based on a detailed survey of a single, representative sand wave. The area under the wave, from the trough of the wave on its downstream side to where the wave appeared flat on its stoss slope, was measured in each profile. Integration of those areas yielded the total volume of the sand wave; division by the crest length gave $V_{0(\min)}$, which can be multiplied by observed crest length to estimate individual sand wave volume. This bulk volume was multiplied by 0.6 to account for porosity (Yalin, 1972). This method accounted for irregularity of wave shapes, gradual disappearance of the waves at their ends and the need to relate measured migration distances of wave crests to sand volumes. $V_{0(\min)}$ was calculated as 15.2 m^3 m^{-1} λ^{-1}.

For a maximum estimate, a 15 cm thick layer of "active sand" is assumed to exist across the interval between wave crests, with a porosity factor of 0.6, so that $V_{0(\max)} = V_{0(\min)} + (0.6)(0.15)\lambda$. This estimate accounts for mobility of the bottom layer: sand is being transported across the entire platform, not simply in the crestal area of large-scale sand waves. Ripples serve as transport mechanisms and are ubiquitous over the platform. The low steepness (wave height/wave length) of the sand waves made the sand-wave shape indistinguishable from the local topography only a few meters from the crest, making it impossible to integrate the sand wave volume across the entire wavelength and necessitating this "active layer" approximation. The 15-cm layer agrees well with the maximum depth of sediment

burial determined by Heathershaw (1981) in a similar environment, based on radioactive tracers. Also the total volume calculated using the $V_{0(max)}$ for a 100-m wave is close to a volume determined using the area under an idealized sand wave of triangular profile, 50 cm in height with a length of 100 m, dimensions typical of sand waves on Popponesset Platform.

Ten-year sediment transport rates were calculated for sand waves A through M (Figs.4 and 5). Maximum and minimum transport rates (m^3 per m of platform width per year) were calculated using the formulas:

$$I_{r(min)} = \frac{V_{0(min)} D}{\lambda}$$

and:

$$I_{r(max)} = \frac{(V_{0(min)} + 0.09\lambda) D}{\lambda}$$

where D = average annual migration distance and λ = wavelength. These normalized rates varied from sand wave to sand wave because of differences in migration distances and wavelengths. Minimum estimates ranged from 0.4 to 2.3 $m^3\ m^{-1}\ yr^{-1}$ and maximum estimates from 1.0 to 3.3 $m^3\ m^{-1}\ yr^{-1}$. Mean values were 1.24 and 2.3 $m^3\ m^{-1}\ yr^{-1}$, respectively, with uncertainty of approximately 0.5 $m^3\ m^{-1}\ yr^{-1}$.

Since these values are normalized by the wavelength, they represent the average volume rate of sand transport past a line on the platform. For example, for a point opposite Popponesset Spit where the platform is about 1 km wide, the transport estimates fall in the range:

$1240\ m^3\ yr^{-1} < V < 2300\ m^3\ yr^{-1}$

PREDICTED SEDIMENT TRANSPORT BASED ON FLOW FIELDS

Application of laboratory-derived, empirical sediment transport formulas to a field situation requires a set of assumptions about the physics of the interactions of the seabed with the flow. We relate our point velocity measurements to bed shear stress using either the Karman-Prandtl logarithmic velocity profile or a drag coefficient. The Shields curve is used to define a threshold shear stress for initiation of motion. The bedload equations used in this study were formulated in laboratory flows generating shear stresses only slightly stronger than necessary for initiation of sediment motion, so they are not appropriate for situations involving suspended transport.

The volume of sediment in suspension can be determined by comparing the shear velocity (u_*) with the fall velocity of the sediment grains (w), in the form:

$$P_s = \frac{w}{\kappa u_*}$$

For values of $P_s > 2$, suspended load is negligible (Smith, 1977); using the

maximum tidal current in the Popponesset area of about 40 cm s^{-1} and the fall velocity of the median grain size, a value of $P_s = 4.64$ is obtained. The bedload criterion is therefore met.

The Shields curve is the most reliable criterion available for initiation of motion on a flat bed, although some investigators have suggested that it underpredicts the threshold velocity in rippled bed environments (Dyer, 1980). The logarithmic velocity profile and drag coefficient relate the current velocity to shear stress on a flat or rippled surface, but they do not account for the effects of large scale features found in natural environments, such as the Popponesset Platform sand waves. An analysis of flow over a wavy bottom (Smith, 1977) to determine the sand waves' effects on the flow, however, showed that these small amplitude waves had a negligible effect on the flow at 150 cm from the bottom where these measurements were made, justifying the rippled flat bed assumption.

Meyer-Peter and Müller model

The Meyer-Peter and Müller (M-PM) bedload formula is a simple, purely empirical method for estimating sediment transport, developed using extensive flume data (Meyer-Peter and Müller, 1948). It is based on the assumption that bedload volume transport is related to boundary shear stress beyond the value necessary for initiation of sediment motion, as expressed in the difference in Shields Parameter values $\psi - \psi_c$. The method has been tested in more recent laboratory studies (Wilson, 1966; Fernandez Luque and Van Beck, 1976) and found to be quite accurate.

To estimate sediment transport rate from flow measurements using this method, the current velocity is converted to a boundary shear stress using the Karman-Prandtl logarithmic velocity profile:

$$\frac{u}{u_*} = \frac{1}{\kappa} \ln \frac{z}{z_0}$$

where u is the velocity measured a distance z from the bottom; κ is von Karman's constant, equal to 0.4; z_0 is a measure of the boundary roughness; and u_* is the shear velocity, equal to $\sqrt{\tau_0/\rho}$; τ_0 is boundary shear stress; ρ is fluid density. The primary roughness elements upon which the value of z_0 depends were assumed to be ripples whose parameters were defined by the median grain size (d) according to Yalin (1972), so that λ_r = ripple length = 1000 d and H = ripple height = 0.1 λ_r. These dimensions were used to determine the Nikuradse equivalent sand-grain roughness, k_b, and thence the roughness length z_0. In rough turbulent flow, the condition at Popponesset during sand transport, z_0 equals $k_b/30$. For a flat bed, the equivalent sand-grain roughness equals the sand-grain diameter, but for a rippled bed it is greater and for current-formed ripples can be defined (Glenn, 1983):

$$k_b = 30H(H/\lambda)$$

For a mean grain size of 35 μm and a rippled bed:

$z_0 = 0.35$ cm

A boundary shear stress can be calculated from each velocity measurement using these formulas. This shear represents the total stress acting on the flow and can be parameterized into a skin friction component and a form drag component according to a drag partitioning scheme (Engelund, 1966). The skin friction, which is responsible for bedload transport, is generated by the interaction of the fluid with the sand grains in the bed. In this case, drag partitioning shows skin friction representing 60% of the total shear stress felt by the flow; Meyer-Peter and Müller (1948) found skin friction over a rippled bed to be 50% of the total. The rest of the shear stress is due to pressure gradients generated by flow over the ripples.

A modified Shields diagram (Madsen and Grant, 1976) was used to determine the critical shear velocity for initiation of grain motion. The critical Shields parameter ψ $[= \tau_0/(s\text{-}1)\rho g d]$ is 3.6×10^{-2}, which translates to a critical shear velocity of 1.41 cm s^{-1}. We assume here that the median grain size for the platform adequately represents the bed.

Each velocity measurement was used to calculate a Shields parameter value. If the calculated Shields parameter was greater than the critical value, volume sediment transport was calculated using the modified M-PM bedload equation:

$$q_{sb} = 8\left[d\sqrt{\left(\frac{\rho_s}{\rho} - 1\right)\rho g d}\right](\psi - \psi_c)^{3/2}$$

This equation can account for partitioning of the total shear stress, but has been changed from the original M-PM to explicitly include the Shields parameter (Wilson, 1966).

To calculate transport rates, the 17-day velocity record was averaged over 640-s intervals and each velocity used to produce a transport estimate. The positive (northeast) and negative (southwest) values were summed separately to provide gross directional transport values, then added together to estimate net transport rates for the period of current meter deployment. Because tidal flows are generally predictable, to first order the 17-day record can be assumed to reflect conditions throughout the year. On this assumption, yearly transport rates were extrapolated from the 17-day transport values (Table I).

The MP-M estimates are strongly dependent on two parameters which may vary with unsteadiness in the flow and irregularities in bedforms: the skin friction/total bed shear stress ratio and the z_0 value. The skin fraction percentage calculated using the Engelund method (60%) and the z_0 value derived from equilibrium bedforms in a steady flow over a uniform sand (0.35 cm) are maximum estimates. The effects of varying these parameters are shown in Table I; the MP-M calculations are particularly sensitive to variations in the skin friction percentage. Even the highest estimates, how-

TABLE I

Calculated sediment transport rates on Popponesset Platform ($m^3\ m^{-1}\ yr^{-1}$)

	Net positive to S.W.	Gross transport rates		
		to NE	to SW	Total
Sandwave volume, minimum	1.24	n.a.	n.a.	n.a.
Sandwave volume, maximum	2.29	n.a.	n.a.	n.a.
Meyer-Peter, Müller (current only)	0.71	0.36	1.07	1.43
% skin friction = 0.5	0.38	0.10	0.48	0.58
% skin friction = 0.4	0.13	0.01	0.14	0.15
z_0 = 0.17	0.32	0.07	0.39	0.46
Meyer-Peter, Müller [current/ wave (ψ_{cr} = 0)]	1.01	1.22	2.24	3.43
Bagnold (current only) $\beta = 4.5 \times 10^4$	0.13	0.07	0.20	0.27
$\beta = 7.2 \times 10^4$	0.21	0.11	0.32	0.43

Meyer-Peter, Müller calculations have the following parameter values, with exceptions as noted: z_0 = 0.35 cm; skin friction/total bed shear = 0.6; ψ_{cr} = 0.035. Bagnold calculations have a critical velocity u_{cr} = 21.0 cm s^{-1} for current only.

ever, are substantially smaller than the minimum volume transport predictions based on sand wave migration. This suggests that currents alone are not responsible for the observed transport, and the effects of storm waves on total transport should be incorporated. This can be accomplished in a general way using long-term wind records with the current measurements.

Since background (non-storm) wave energy is low, daily wave activity has little or no effect on the boundary shear stress. A sustained wind of greater than 15 knots (7.5 m s^{-1}), however, increases local significant wave heights to 1.0 m or more, with periods of more than four seconds. Applying the Grant and Madsen (1979) model for boundary shear stress due to combined wave and current activity shows waves of this size increase the shear stress above the critical value for all values of current velocity. Under the assumption that current measurements represent the driving force for sediment transport even during storms, with waves having only the effect of increasing bed shear stress to make sediment available for transport, storm-generated transport can be estimated.

Calculations using the M-PM formula were repeated with the critical Shields parameter set to zero, assuming wave shear stress is sufficient to initiate sediment motion. A physical limitation to this approach is its neglect of the non-linear effects of wave/current interaction (Grant and Madsen, 1979), a problem which is compounded when the M-PM equation is linearized by simply dropping the critical Shields parameter. The estimates, therefore, can be viewed only as first-order approximations of the effects of waves on sediment transport. Likewise, values of z_0 and skin friction/total shear change as bedforms are washed out by increased wave stress, but for the purpose of this rough comparison they will be left constant. National weather service records show wind velocities greater than 7.5 m s^{-1} approxi-

mately 22% of the time, so transport rate estimates are based on combined wave/current shear stresses 22% of the year, with tidal currents alone determining the remainder.

These predicted rates fall much closer to the transport rates calculated from sand wave migration (Table I). These wave/current estimates give a rough indication of the effects of wave action on boundary shear stress and sediment transport, demonstrating that excess transport calculated by sand wave migration can be explained partly by storm wave action. The calculations reflect several simplifying assumptions: that effects of changes in bed roughness due to increased shear stress are negligible; that transport rates based on laboratory-developed bedload models for unidirectional flow are representative of wave-dominated conditions in the field; that the M-PM equation can be linearized as described above; and that currents during storms are well-represented by our 17-day record, rather than depending on storm setup. While the closer agreement with observed rates demonstrates the potential importance of storm waves even in this sheltered, tidally dominated environment, specific transport values are only estimates.

Bagnold model

The Bagnold model rests on the assumption that the volume of bedload transport is proportional to the stream power per unit area of the bed lost due to friction between the fluid and the bed (Bagnold, 1963). The power per unit area can be expressed in terms of the boundary shear velocity cubed (Inman et al., 1966), which can be related to current velocity to calculate transport estimates from current meter data. Other studies (Gadd et al., 1978; Heathershaw, 1981) have applied the Bagnold sediment transport equation to nearshore current measurements; Heathershaw (1981) also compared predictions with transport rates based on tracer dispersion. The Bagnold formula was modified by Gadd et al. (1978) to incorporate a threshold shear stress. Using flume data from Guy et al. (1966), they express the original Bagnold equation in terms of the velocity one meter above the bed, U_{100}, and a critical current velocity U_{cr}:

$$q_{sb} = \frac{\beta}{\rho_s} (U_{100} - U_{cr})^3$$

The empirical coefficient of proportionality β, determined from the flume data, incorporates the drag coefficient $C_{d100} = 3.1 \times 10^{-3}$. Values of β ranged from 7.22×10^{-5} to 1.73×10^{-5} g cm^{-4} s^2 for d_{50} equal to 190 and 450 μm, respectively, with a mean value of 4.48×10^{-5} g cm^{-4} s^2. The mean and larger values were used in our calculations.

The logarithmic velocity profile was used to determine U_{100} from measurements at $z = 150$ cm, with the critical U_{100} obtained from the Shields diagram. The critical velocity obtained in this manner is 21 cm s^{-1}, based on the median grain size for the platform.

Gross and net transport rates were calculated in the same manner used for the MP-M method. The values determined from the 640-s average current velocities (Table I) are substantially lower than the M-PM rates, but within the same order of magnitude and in the same direction. Variation of the skin friction/total shear ratio in the M-PM calculations can bring them into near agreement.

CONCLUSIONS

This study has several implications for the study of sediment transport in the nearshore environment. First, results provide a rough corroboration of laboratory-derived sediment transport formulas for field situations on time scales of years to decades. Measured and theoretical estimates determined in this study are the same order of magnitude and in the same direction. Given the uncertainties and assumptions, this agreement is encouraging. The rough agreement between the Meyer-Peter and Müller and Bagnold calculations for unidirectional, steady flow strengthens this argument since both Heathershaw (1981) and Gadd et al. (1978) found the Bagnold formula to be the most accurate for prediction of bedload transport. Partitioning of the total boundary shear stress into skin friction and form drag components was critical to the M-PM estimates, however, and the assumptions made in partitioning are rather uncertain. The variability introduced by changing the skin friction/form drag ratio emphasizes the need for a reliable method for measuring or calculating the shear stress on a rippled bed. The Meyer-Peter and Müller equation is useful for examining the effects of variation of different parameters on transport estimates since it makes the calculation more responsive to a particular flow. As flow conditions can be more accurately measured and their interactions with the seafloor better understood, this method should become more widely used.

Secondly, the study demonstrates the importance of wave action in any nearshore environment. Wave energy is generally very low on this sheltered, shallow platform; but infrequent, high-energy storms are critical to modeling net transport of sediment, even in a tidally dominated region of this sort.

Finally, this study has demonstrated the utility of long-term photographic coverage of shallow, nearshore regions floored by large bedforms. Bedform migration rates, under suitable water conditions and depths, can be documented better from these photographs than from repeated bathymetric profiling or tracer studies.

Theory and measurement techniques must undergo numerous changes and advances before accurate sediment transport predictions can be confidently made from measurements of waves, currents and grain size. The agreement between theory and measurements of net transport demonstrated in this study, however, is an encouraging measure of the convergence of field and lab techniques over time scales of interest to scientists and engineers.

ACKNOWLEDGEMENTS

The research described in this paper was supported by the Town of Mashpee, Mass., a Community Assistance Grant from the Massachusetts Coastal Zone Management Program, the Woods Hole Oceanographic Institution Sea Grant Program Grant No. NA80AA-D-00077(RB-40), the Woods Hole Oceanographic Institution Coastal Research Center and the Alcoa Foundation. We would like to thank Mr. Steve Gegg of W.H.O.I. for his support in the field work and programming. We also thank Pam Barrows for her help in preparation of this paper. Woods Hole Oceanographic Institution Contribution No. 5669. Thomas M. Brocher, William D. Grant and John D. Milliman provided helpful comments on the manuscript.

APPENDIX

Key to symbols

C_{d100} = drag coefficient relating current velocity at z = 100 cm to boundary shear stress
d = mean sand-grain size (cm)
D = average annual sand-wave migration distance (m)
E = total wave energy per unit area (dyne cm^{-2})
g = gravitational acceleration
H = ripple height (cm)
$H_{1/3}$ = significant wave height (cm)
I_r = volume sediment transport rates (m^3 m^{-1} yr^{-1})
k_b = Nikuradse equivalent sand-grain roughness (cm)
q_{sb} = bedload transport rates of sediment (cm^3 m^{-1} yr^{-1})
s = relative density of the sediment particle ρ_s/ρ
u = measured current velocity (cm s^{-1})
u_* = shear velocity = τ_0/ρ (cm s^{-1})
U_{100} = current velocity 100 cm above the bed (cm s^{-1})
U_{cr} = critical U_{100} for initiation of sediment motion
V = volume rate of sediment transport (m^3 yr^{-1})
V_0 = reference sand-wave volume (m^3 m^{-1} λ^{-1})
w = sediment grain fall velocity (cm s^{-1})
z = distance above seafloor (cm)
z_0 = boundary roughness length (cm)
$\langle \eta^2 \rangle$ = wave-energy variance (cm^2)
β = coefficient of proportionality in Bagnold formula (g cm^{-4} s^2)
η = displacement of the free surface from mean sea level, due to surface waves (m)
κ = Von Karman's constant
λ = wavelength of sand wave (m)
λ_r = ripple length (cm)
ρ = fluid density (g cm^{-3})
ρ_s = sediment density (g cm^{-3})
τ_0 = boundary shear stress (dyne cm^{-2})
ψ = Shields parameter = $\tau_0/[(s\text{-}1)\,\rho g d]$

REFERENCES

Aubrey, D.G., 1979. Seasonal patterns of on/offshore sediment movement. J. Geophys. Res., 84: 6347—6354.

Aubrey, D.G. and Gaines, A.G., 1982. Recent evolution of an active barrier beach complex: Popponesset Beach, Cape Cod, Mass. Woods Hole Oceanogr. Inst., Tech. Rep., WHOI-82-3: 77 pp.

Aubrey, D.G. and Goud, M.R., 1983. Coastal sediment transport: Popponesset Beach, MA. Woods Hole Oceanogr. Inst., Tech. Rep., WHOI-83-26: 132 pp.

Bagnold, P.A., 1963. Mechanics of marine sedimentation. In: M.N. Hill (Editor), The Sea, 3. Wiley, New York, N.Y., pp.507—582.

Bokuniewicz, H.J., Gordon, R.B. and Kastens, K.A., 1977. Form and migration of sand waves in a large estuary, Long Island Sound. Mar. Geol., 24: 185—199.

Dyer, K.R., 1980. Velocity profiles over a rippled bed and the threshold of movement of sand. Estuarine Coastal Mar. Sci., 16: 181—199.

Engelund, F., 1966. Hydraulic resistance of alluvial streams. J. Hydraul. Div., Am. Soc. Civ. Eng., 92 (HY2): 315—326.

Fernandez Luque, R. and Van Beck, R., 1976. Erosion and transport of bed-load sediment. J. Hydraul. Res., 14: 127—144.

Gadd, P.E., Lavelle, J.W. and Swift, D.J.P., 1978. Estimates of sand transport on the New York Shelf using near-bottom current meter observations. J. Sediment. Petrol., 48: 239—252.

Gilbert, G.K., 1914. The transportation of debris by running water, based on experiments made with the assistance of E.C. Murphy. U.S. Geol. Surv., Prof. Pap. 86, 263 pp.

Glenn, S.M., 1983. A continental shelf bottom boundary layer model: the effects of waves, currents and a moveable bed. Ph.D. Thesis, Woods Hole Oceanographic Institution, Woods Hole, Mass.

Gonella, J., 1972. A rotary-component method for analyzing meteorological and oceanographic vector time series. Deep-Sea Res., 19: 833—846.

Grant, W.D. and Madsen, O.S., 1979. Combined wave and current interactions with a rough bottom. J. Geophys. Res., 84: 1797—1808.

Grant, W.D. and Madsen, O.S., 1982. Moveable bed roughness in unsteady oscillatory flow. J. Geophys. Res., 87: 469—481.

Guy, H.P., Simons, D.B. and Richardson, E.V., 1966. Summary of alluvial channel data from flume experiments 1955—1961. U.S. Geol. Surv., Prof. Pap. 4621, 92 pp.

Heathershaw, A.D., 1981. Comparisons of measured and predicted sediment transport rates in tidal currents. Mar. Geol., 42: 75—104.

Inman, D.L., 1952. Measures for describing the size distribution of sediments. J. Sediment. Petrol., 22: 145—152.

Inman, D.L., Ewing, G.C. and Corliss, J.B., 1966. Coastal sand dunes of Guerrero Negro, Baja, California, Mexico. Geol. Soc. Am. Bull., 77: 787—802.

Komar, P.D. and Inman, D., 1970. Longshore sand transport on beaches. J. Geophys. Res., 75: 5914—5927.

Madsen, O.S. and Grant, W.D., 1976. Sediment transport in the coastal environment. Ralph M. Parsons Lab. Rep. 209, Mass. Inst. Tech., 105 pp.

McCave, I.N., 1971. Sand waves in the North Sea off the coast of Holland. Mar. Geol., 10: 199—225.

Meyer-Peter, E. and Müller, R., 1948. Formulas for bedload transport. Proc. 2nd Meet., Mtl. Assoc. Hydraulic Struct. Res., Append. 2: 39—64.

Salsman, G.G., Tolbert, W.H. and Villars, R.G., 1966. Sand wave migration in St. Andrew Bay, FL. Mar. Geol., 4: 11—19.

Schlee, J., 1966. A modified Woods Hole rapid sediment analyzer. J. Sediment. Petrol., 36: 403—413.

Simons, D.B. and Richardson, E.V., 1961. Forms of bed roughness in alluvial channels. Proc. Am. Soc. Civ. Eng., 87 (HY3): 87—105.

Smith, J.D., 1977. Modeling of sediment transport on continental shelves. In: E.D. Goldberg, I.N. McCave, J.J. O'Brien and J.H. Steele (Editors), The Sea. Wiley-Interscience, New York, N.Y., pp.539—577.

Wilson, K.C., 1966. Bed-load transport at high shear stress. Proc. ASCE, J. Hydraul. Div., 92 (HY6): 49.

Yalin, M.S., 1972. Mechanics of Sediment Transport. Pergamon, Oxford, 290 pp.